Communications in Mathematics and Applications
Vol. 15, No. 5, pp. 1595–1606, 2024
ISSN 0975-8607 (online); 0976-5905 (print)
Published by RGN Publications
DOI: 10.26713/cma.v15i5.2845

http://www.rgnpublications.com

Research Article

Analysis of Ree-Eyring Fluid Flow With Heat Transfer and Irreversibility Characteristics Over a Stretching Sheet With Variable Thermal Conductivity: A Couple Stress Model

Gopinath Veeram[1], Tailam Venkata Gayatri[2], G. V. Ramana*[3], M. Srikanth[3], Darapuneni Purna Chandar Rao[4] and B. Purushotham[5]

[1] *Department of Mathematics, Ch. S. D. St. Theresa's College for Women (A), Eluru 534003, Andhra Pradesh, India*
[2] *Department of Mathematics, Sir C. R. R. College of Pharmaceutical Sciences (A), Eluru 534003, Andhra Pradesh, India*
[3] *Department of Mathematics, Aditya University, Surampalem 533437, Andhra Pradesh, India*
[4] *Department of Mathematics, Matrusri Engineering College, Saidabad, Hyderabad 500059, Telangana, India*
[5] *Department of Mathematics, Government Degree College, Rajampeta, Annamayya 516115, Andhra Pradesh, India*
***Corresponding author:** ramanaginjala9@gmail.com

Received: August 5, 2024 **Accepted:** November 13, 2024

Abstract. Ree-Eyring fluids are good models for lubricants. Understanding the flow behavior of these fluids under stretching conditions can help design better lubricants for applications like bearings and gears, especially at varying shear rates. This research delves into the aspects of heat transmission and magnetohydrodynamic movement of the Ree-Eyring fluid across an elastic sheet. The effect of numerous factors on the fluid's properties, including temperature, is investigated. The equations governing the problem are subjected to transformation and processed with the bvp5c solver. The findings reveal that a stronger magnetic field impedes the fluid flow. Conversely, a higher Ree-Eyring parameter and a higher couple stress parameter promote faster flow rates. The study demonstrates that the Eckert number and heat source parameter contribute to an upsurge in fluid temperature. In contrast, a higher Prandtl number signifies stronger thermal diffusivity, resulting in a lower temperature profile. A higher Brinkman number indicates a more significant role for viscous dissipation, leading to increased entropy generation. The Bejan number, which reflects the relative dominance of heat transmission versus viscous dissipation, decreases with a rise in viscous dissipation. Finally, the study presents mathematical relationships that quantify the impression of these parameters on the friction factor and Nusselt number.

Keywords. Non-Newtonian fluid, bvp4c, Couple stress, Viscous dissipation, Entropy generation, Magnetic field

Mathematics Subject Classification (2020). 76A05, 76D05

1. Introduction

The importance of non-Newtonian fluid flow across an elastic sheet stems from its connection to real-world applications and its role as a simplified model for complex flows. By studying the flow of a non-Newtonian flow across an elastic sheet, engineers can improve industrial process design and efficiency, enhance product quality and consistency, and develop better predictive models for complex flow situations. In their numerical study, Javed and Ghaffari [8] used the shooting method to examine the Maxwell fluid flow through an elastic sheet near a slant-ing stagnation point. A higher value of the shearing parameter is associated with a faster fluid velocity. Sajjad-ur-Rehman *et al*. [21] addressed the three-dimensional Casson fluid flow across an exponentially stretched surface in their discussion of the HAM approach. They observe an escalation in the temperature profile as the Casson fluid parameter upsurges. Ibrahim *et al*. [6] studied the thermal characteristics of two types of fluid flows, Casson and Williamson, across a stretched surface with heat source and Dufour parameters. When comparing the temperature profiles of Williamson and Casson fluids, it is shown that the heat source parameter significantly improves the former. The flow of Walter's B fluid through a permeable plate with nonconstant viscosity was studied by Hussain *et al*. [5]. As the Prandtl number rises, it is found that the fluid's temperature declines. Building on the previous work, Idowu and Falodun [7] included Casson fluid and cross-diffusion effects. Using the HAM method, Khan *et al*. [10] investigated the Carreau fluid's three-dimensional flow via a porous elastic surface subjected to cross-diffusion effects. A decrease in fluid velocity is observed when the Weissenberg number increases. Using velocity slip, Sharma and Shaw [25] examined two types of fluid flows (Williamson and Casson) across an uneven elastic surface. It has been noted that the surface drag is reduced by the velocity slip. Subsequently, a number of scholars (Faghiri *et al*. [4], Maranna *et al*. [14], Biswal *et al*. [3], Shahzad *et al*. [23], and Rehman *et al*. [20]) engaged in the examination of diverse non-Newtonian fluid flows across different geometries.

Studying flow over a stretching sheet can provide insights into the mass transfer and heat transfer during the growth of crystals from solutions. This knowledge can be used to control crystal size, morphology, and uniformity, leading to improved material properties. Mahanthesh *et al*. [13] inspected the convective flow of a nanofluid in the slip regime. A significant influence of the slip circumstances on the boundary layer is observed. Using thermophoresis and the *Homotopy Analysis Method* (HAM), Rasool *et al*. [19] examined the nanofluid's non-Darcy flow. There is a negative correlation between porosity and flow momentum. Using slip parameters, Sreedevi *et al*. [26] inspected the hydrodynamic flow of a hybrid nanofluid through an elastic surface. They noticed that an upsurge in the slip parameter (related to velocity) corresponds to a drop in the temperature of the fluid. In order to discuss two types of fluid flows (including Jeffrey) across an elastic sheet, Sarada *et al*. [22] conducted an investigation using the shoot method. The velocity profile of Oldroyd-B fluid decreases at a greater rate than that of Jeffrey fluid when the magnetic field increases. Khan *et al*. [9] examined the Maxwell fluid flow through an elastic sheet with cross-diffusion effects. As the unstable parameter increases, the reduction of the temperature profile is noted. Using the DTM-pade approach, Muntazir *et al*. [16] investigated the two nanofluids' aquatic flow over a porous stretched sheet subjected to viscous dissipation. Arshad *et al*. [2] conducted a numerical analysis to examine the spinning motion of hybrid

nanofluids using the bvp4c solver. The hybrid nanofluid plays a significant role in heat transfer when a magnetic field is present. Ariffin *et al*. [1] scrutinized the influence of the suction on the Reiner-Philippoff fluid flow in the slip regime. It has been determined that both slip parameters have an equal effect on the Nusselt number. Subsequently, a number of scholars (Patil *et al*. [17], Lone *et al*. [12], Mohana *et al*. [15], Khan *et al*. [11], and Shahzad *et al*. [24]) engaged in the examination of diverse fluid flows across stretching sheet.

Ree-Eyring fluids are good models for lubricants, and understanding their flow behavior is crucial for designing better lubricants (e.g., for bearings and gears). Studying flow over an elastic sheet simplifies complex flows and has applications in crystal growth control. This study aims to bridge the gap in our understanding of Ree-Eyring fluid flow under a magnetic field by analyzing its *magnetohydrodynamic* (MHD) flow and heat transfer characteristics over a stretching sheet with variable thermal conductivity and non-uniform heat source parameters using a couple stress model. The effect of numerous factors on the fluid's properties, including temperature, is investigated.

2. Formulation of the Problem

This study theoretically inspects the flow of a Ree-Eyring fluid with variable thermal conductivity and activation energy parameters. The flow occurs via an elastic sheet with the couple stress model. Assumptions underlying the current inquiry are as follows:

(i) The fluid moving across the surface of the sheet at an extending velocity $u_w = bx$ (refer to Figure 1).

(ii) A vertically imposed external magnetic field of strength B_0 affects the flow.

(iii) We do not take into account the effect of stimulated magnetic field in this study.

Given the aforementioned presumptions, the appropriate conditions and fundamental equations required for this investigation are outlined below:

$$v_y + u_x = 0, \text{ i.e., } \frac{\partial v}{\partial y} + \frac{\partial u}{\partial x} = 0, \tag{1}$$

$$\left.\begin{aligned} u\frac{\partial u}{\partial x} + v\frac{\partial u}{\partial y} &= \frac{1}{\rho}\left(\mu + \frac{1}{\chi d}\right)\left(2\frac{\partial^2 u}{\partial x^2} + \frac{\partial^2 v}{\partial x \partial y} + \frac{\partial^2 u}{\partial y^2}\right) + g\beta_C(C - C_\infty) \\ &- \frac{\gamma_0}{\rho}\frac{\partial^4 u}{\partial y^4} + g\beta_T(T - T_\infty) - \frac{\sigma B_0^2}{\rho}u \end{aligned}\right\}, \tag{2}$$

$$u\frac{\partial T}{\partial x} + v\frac{\partial T}{\partial y} = \frac{1}{\rho C_p}\frac{\partial}{\partial y}\left(k(T)\frac{\partial T}{\partial y}\right) + \frac{1}{\rho C_p}\left(\mu + \frac{1}{\chi d}\right)\left(\frac{\partial u}{\partial y}\right)^2 + q''', \tag{3}$$

$$u\frac{\partial C}{\partial x} + v\frac{\partial C}{\partial y} = D_m\frac{\partial^2 C}{\partial y^2} - k_0^2\left(\frac{T}{T_\infty}\right)^m \exp\left(-\frac{E_0}{k_1 T}\right)(C - C_\infty), \tag{4}$$

$$\left.\begin{aligned} &v = 0,\ u = u_w = bx,\ u_{yy} = \frac{\partial^2 u}{\partial y^2} = 0,\ T = T_w,\ C = C_w \text{ at } y = 0 \text{ and} \\ &u \to 0,\ u_y = \frac{\partial u}{\partial y} \to 0,\ T \to T_\infty,\ C \to C_\infty \text{ as } y \to \infty \end{aligned}\right\} \tag{5}$$

Note that

$$k(T)=k_\infty\left(1+\varepsilon\frac{T-T_\infty}{T_w-T_\infty}\right),\quad q'''=\frac{k(T)b}{\upsilon}\left[Q(T-T_\infty)+Q^*(T_w-T_\infty)\exp\left(-y\sqrt{\frac{b}{\upsilon}}\right)\right].$$

Here $Q,Q^*,\rho,\gamma_0,k(T),\sigma,C_p,D_m,k_1$, and E_0 represents heat source, fluid density, couple stress coefficient, electrical conductivity, thermal conductivity, specific heat capacity, molecular diffusivity, Boltzmann constant and activation energy parameters respectively.

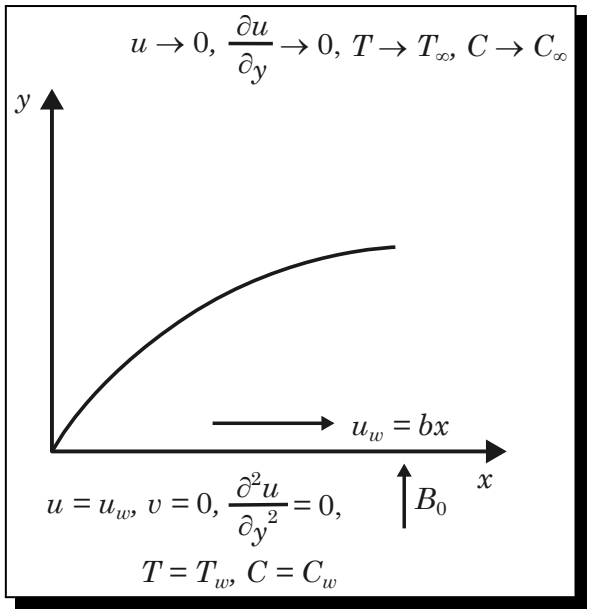

Figure 1. Diagrammatical representation of the present study

Rao *et al*. [18] presented subsequent similarity transmutations for the conversion of regulating equations:

$$\left.\begin{aligned}&\eta=y\sqrt{\frac{u_w}{\upsilon x}},\quad u=bxf'(\eta)=u_wf'(\eta),\quad T=T_\infty+\theta(\eta)(T_w-T_\infty),\\&v=-(\upsilon b)^{0.5}f(\eta),\quad C=C_\infty+\Phi(\eta)(C_w-C_\infty).\end{aligned}\right\}. \tag{6}$$

Equation (1) can be easily fulfilled by using (6). Equations (2)-(4), as well as condition 5, can be effectively modified by integrating (6) in the ensuing process:

$$(1+We)f'''-Csf^{V}+ff''-f'^2+\lambda\theta+\lambda\lambda_1\Phi-Mgf'=0, \tag{7}$$

$$\frac{1}{Pr}(1+\varepsilon\theta)\theta''+\frac{1}{Pr}\varepsilon\theta'^2+f\theta'+\frac{1}{Pr}(1+\varepsilon\theta)(Q\theta+Q^*\exp(-\eta))+(1+We)Ecnf''^2=0, \tag{8}$$

$$\frac{1}{St}\Phi''+f\Phi'-\Gamma(1+\alpha\theta)^m\exp\left(-\frac{Eg}{1+\alpha\theta}\right)\Phi=0, \tag{9}$$

$$\left.\begin{aligned}&f(0)=0,\ f'(0)=1,\ f'''(0)=0,\ \theta(0)=1,\ \Phi(0)=1,\ \text{i.e., at } \eta=0,\\&f'(\infty)\to 0,\ f''(\infty)\to 0,\ \theta(\infty)\to 0,\ \Phi(\infty)\to 0,\ \text{i.e., as } \eta\to\infty\end{aligned}\right\}, \tag{10}$$

where Eckert number (Ecn), Schmidt number (St), Weissenberg number (We), Reynolds number (Re_x), Reaction rate parameter (Γ), Grashoff number (Gr), Couple stress parameter (Cs), Mixed convection parameter (Ri), Prandtl number (Pr), Magnetic parameter (Mg), Activation energy

parameter (Eg), Temperature difference parameter (α) are outlined as:

$$\left.\begin{aligned} &We = \frac{1}{\mu\chi d},\ Re_x = \frac{xu_w}{\upsilon},\ St = \frac{\upsilon}{D_m},\ Gr = \frac{g\beta_T(T_w - T_\infty)x^3}{\upsilon^2},\ \lambda = \frac{Gr}{Re_x^2},\ Ecn = \frac{u_w^2}{C_p(T_w - T_\infty)},\\ &Pr = \frac{\mu C_p}{k},\ Cs = \frac{\gamma_0 b}{\rho\upsilon^2},\ Mg = \frac{\sigma B_0^2}{\rho b},\ \Gamma = \frac{k_0^2}{b},\ \alpha = \frac{T_w - T_\infty}{T_\infty},\ Gc = \frac{g\beta_C(C_w - C_\infty)x^3}{\upsilon^2},\ \lambda_1 = \frac{Gc}{Gr}. \end{aligned}\right\}$$

Heat, mass transmission rates and friction factor are specified as:

$$Nu = \left.\frac{xq_w}{k_\infty(T_w - T_\infty)}\right|_{y=0},\quad Cf = \left.\frac{\tau_w}{\frac{1}{2}\rho u_w^2}\right|_{y=0},\quad Sh = \left.\frac{xs_w}{D_m(C_w - C_\infty)}\right|_{y=0}, \tag{11}$$

where $q_w = -k(T)\frac{\partial T}{\partial y}$, $\tau_w = 2\left(\mu_f + \frac{1}{\chi d}\right)\frac{\partial u}{\partial y}$, $s_w = -D_m\frac{\partial C}{\partial y}$.

The components in (11) can be reconstructed via (6) as:

$$(Re_x)^{-\frac{1}{2}}Nu = -(1+\varepsilon\theta)\theta'(0),$$

$$(Re_x)^{\frac{1}{2}}Cf = 2(1+We)f''(0),$$

$$(Re_x)^{-\frac{1}{2}}Sh = -\Phi'(0).$$

2.1 Irreversibility

Entropy generation in fluid dynamics pertains to the inevitable escalation in the chaos or unpredictability present in a fluid system. Entropy consistently exhibits an upward tendency in practical situations, unlike certain other qualities that may vary. This phenomenon is intricately linked to the Second Law of Thermodynamics, which states that the total entropy of a closed system always increases with time. Minimizing entropy generation often leads to increased energy efficiency. By delving into this subject, engineers can enhance their ability to create more effective pumps, turbines, heat exchangers, and other fluid systems.

The dimensional expression for calculating the total irreversibility in the current flow problem is articulated by the following formula:

$$S_g = \frac{1}{T_\infty^2}k(T)\left(\frac{\partial T}{\partial y}\right)^2 + \frac{1}{T_\infty}\mu\left(\frac{\partial u}{\partial y}\right)^2 + \frac{1}{T_\infty}\sigma u^2 B_0^2 + \frac{\widetilde{R}D_m}{C_\infty}\left(\frac{\partial C}{\partial y}\right)^2 + \frac{\widetilde{R}D_m}{T_\infty}\frac{\partial C}{\partial y}\frac{\partial T}{\partial y}. \tag{12}$$

The following rewriting of equation (12) is possible with the use of (6):

$$Eg = (1+\varepsilon\theta)\alpha\theta'^2 + Brf''^2 + MgBrf'^2 + J\frac{\beta}{\alpha}\Phi'^2 + J\Phi'\theta', \tag{13}$$

where

$$Eg = \frac{\upsilon T_\infty S_g}{b(T_w - T_\infty)k_\infty},\quad Br = \frac{\mu u_w^2}{(T_w - T_\infty)k_\infty},\quad J = \frac{\widetilde{R}D_m(C_w - C_\infty)}{k_\infty},\quad \beta = \frac{C_w - C_\infty}{C_\infty}.$$

To find the Bejan number, one can use the following formula:

$$Be = \frac{\text{The process of entropy formation due to the transfer of mass and heat}}{\text{The overall generation of entropy}}.$$

Applying (13) in the following way allows us to revise Be:

$$Be = \frac{(1+\varepsilon\theta)\alpha\theta'^2 + J\frac{\beta}{\alpha}\Phi'^2 + J\Phi'\theta'}{(1+\varepsilon\theta)\alpha\theta'^2 + Brf''^2 + MgBrf'^2 + J\frac{\beta}{\alpha}\Phi'^2 + J\Phi'\theta'}.$$

3. Discussion of Outcomes

3.1 Profiles of Temperature, Velocity and Concentration

The in-built function bvp4c in MATLAB is employed to resolve equations (7)-(9) with the constraints (10). Figure 2 displays that the escalation in the magnetic field parameter leads to the decrease in the velocity of the fluid. As the magnetic field parameter (which signifies the strength of the magnetic field) increases, the Lorentz force becomes stronger. This stronger opposing force leads to a decrease in the overall fluid velocity. When the Ree-Eyring parameter increases, it indicates a decrease in the fluid's internal resistance to flow. This allows the fluid particles to move more freely, resulting in a higher overall fluid velocity (see Figure 3). When the value of upsurges, it essentially allows the fluid to resist rotational forces more effectively. This can counter the internal friction within the fluid, leading to a faster flow rate (see Figure 4). When the Eckert number increases, it indicates a more significant contribution of kinetic energy. This translates to more energy being converted into thermal energy due to friction between fluid molecules. Consequently, the fluid's temperature rises (see Figure 5). The amount of heat energy added to the fluid is proportional to the value of the heat source parameter. The molecules of the fluid are stirred up by this extra energy, which makes them vibrate with greater intensity. This increased vibration translates to a rise in the average thermal energy of the molecules, which is reflected in a higher fluid temperature (see Figure 6). A lower temperature profile is observed when the Prandtl number increases, as can be seen in Figure 7. Figure 8 clearly establishes that increasing the activation energy parameter leads to a rise in the fluid concentration. When the activation energy is increased, the pace of the reaction decreases, resulting in a smaller reduction of nanoparticles and therefore a higher concentration in the fluid. Figure 9 reveals that augmenting the reaction rate parameter results in a decrease in the fluid concentration.

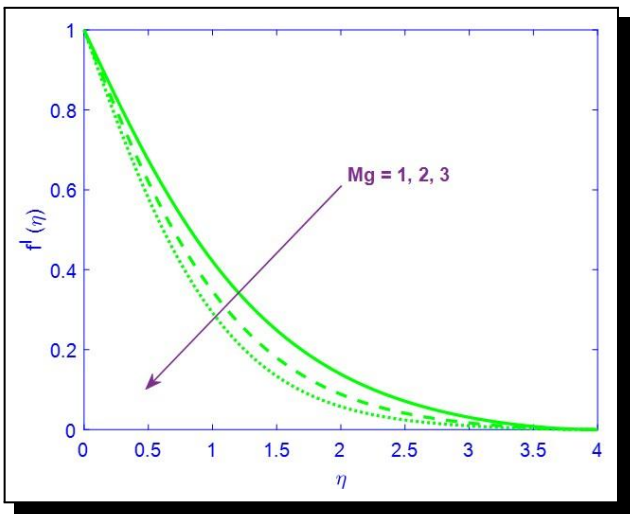

Figure 2. Situation where Mg influences $f'(\eta)$

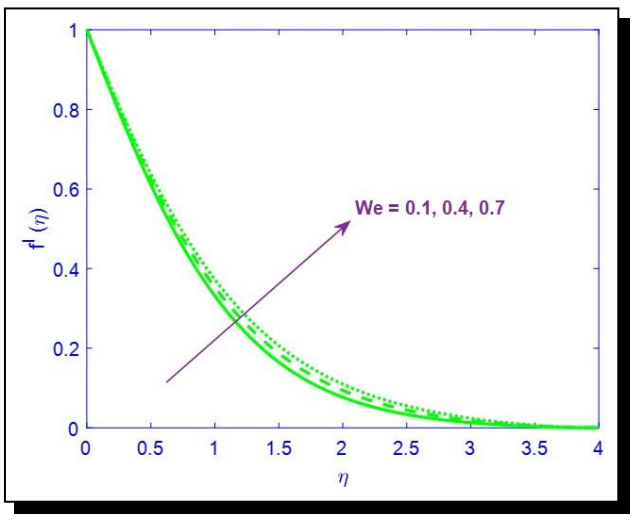

Figure 3. Situation where We influences $f'(\eta)$

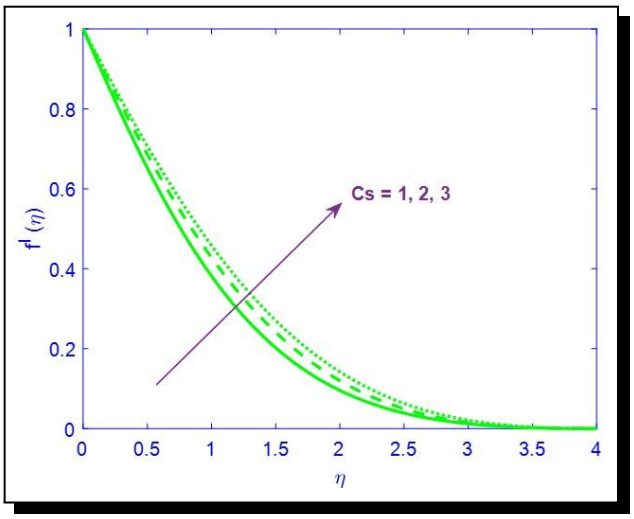

Figure 4. Situation where Cs influences $f'(\eta)$

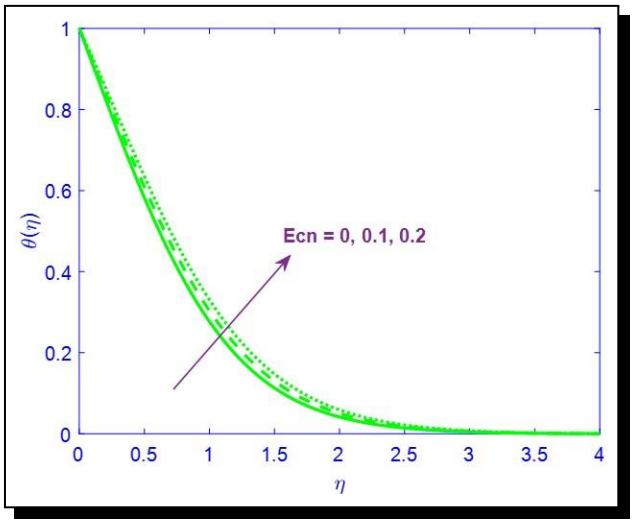

Figure 5. Situation where Ecn influences $\theta(\eta)$

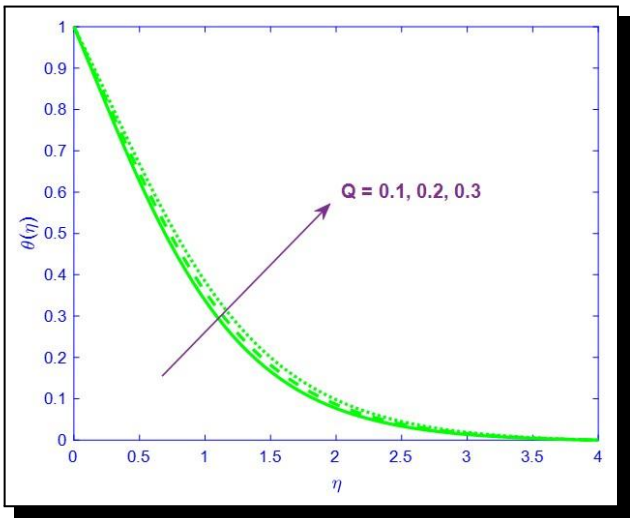

Figure 6. Situation where Q influences $\theta(\eta)$

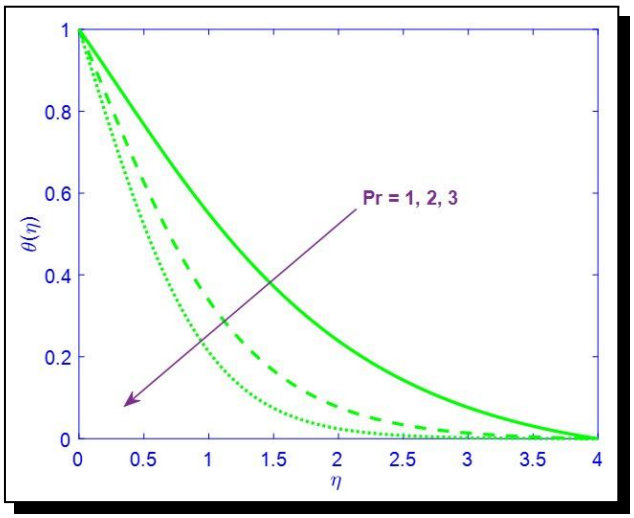

Figure 7. Situation where Pr influences $\theta(\eta)$

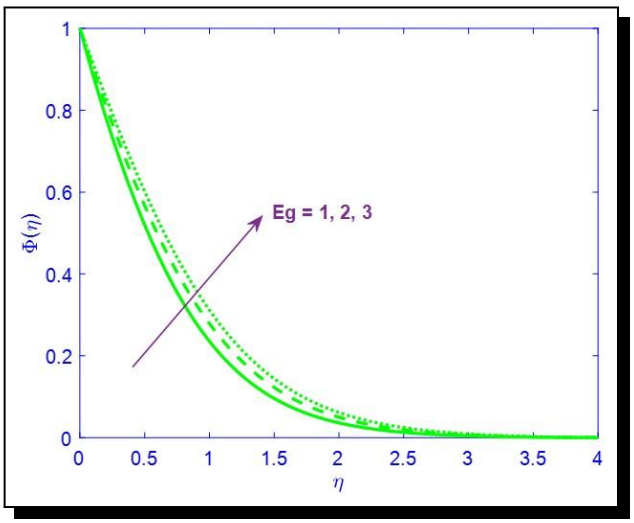

Figure 8. Situation where Eg influences $\Phi(\eta)$

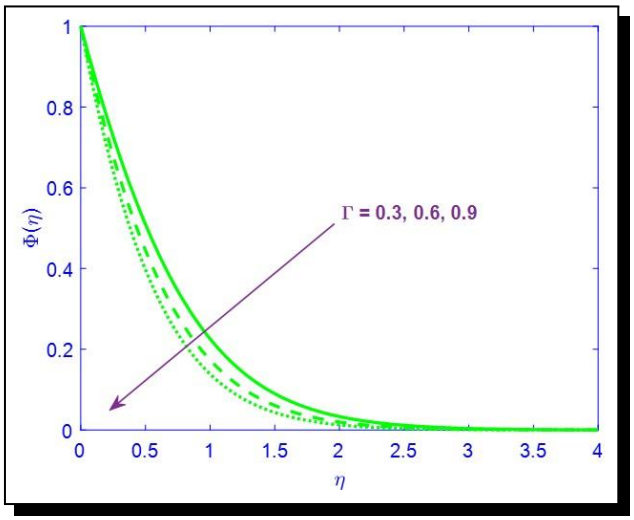

Figure 9. Situation where Γ influences $\Phi(\eta)$

3.2 Irreversibility Analysis

A higher Brinkman number indicates a larger proportion of heat generated by viscous heating in comparison to conductive heat transfer. This leads to increased internal heat production caused by friction, leading to a more substantial increase in entropy (see Figure 10). Based on Figure 11, it is evident that there is a fall in the Bejan number as the Br value increases. It should be noted that a rise in Br (resulting in greater viscous dissipation) leads to a higher total entropy generation within the fluid flow. The increased Ree-Eyring fluid parameter leads to more viscous dissipation. Hence, entropy generation rises (see Figure 12). The increased Ree-Eyring fluid parameter leads to more viscous dissipation. Due to the increased significance of viscous dissipation relative to thermal transfer, the Bejan number decreases (see Figure 13).

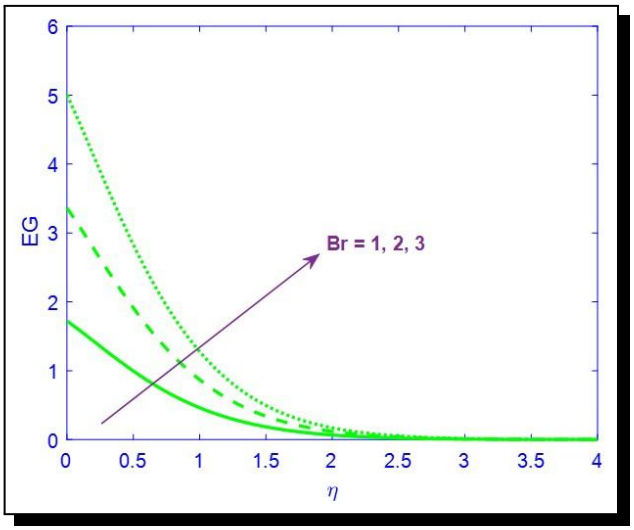

Figure 10. Situation where Br influences Eg

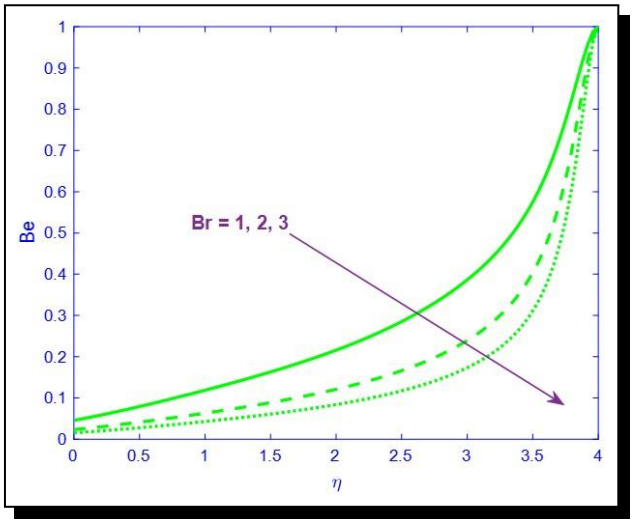

Figure 11. Situation where Br influences Be

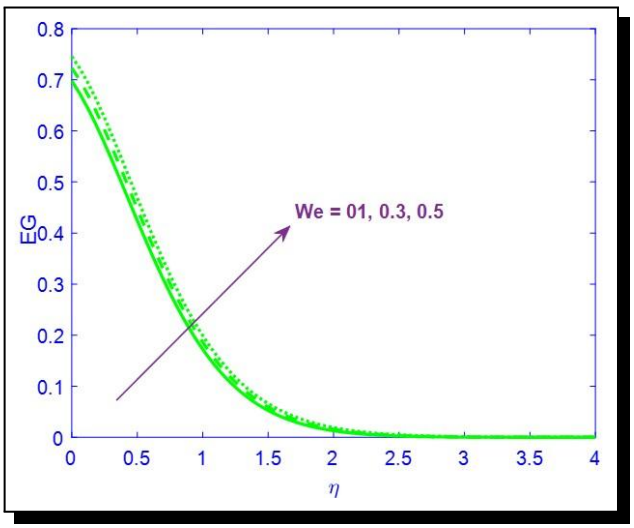

Figure 12. Situation where We influences Eg

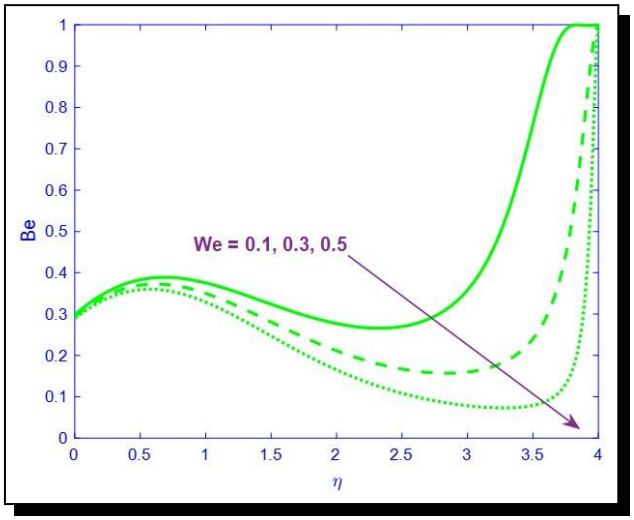

Figure 13. Situation where We influences Be

3.3 Multiple Linear Regression (MLR)

Multiple Linear Regression predicts the value of a dependent variable based on the values of multiple independent variables. MLR builds a linear equation to represent the relationship. This equation includes coefficients for each independent variable, indicating the strength and direction of their influence on the dependent variable.

To establish connections amongst crucial technical attributes like Nusselt number and particular variables like couple stress parameter, this research used the following models:

$$Cf = p_0 + p_1 We + p_2 Mg + p_3 Cs, \tag{14}$$

$$Nu = q_0 + q_1 Q + q_2 Ecn + q_3 Pr, \tag{15}$$

$$Sh = r_0 + r_1 Eg + r_2 \Gamma. \tag{16}$$

In order to accelerate the process of obtaining findings, we employed twenty unique sets of varying values for each computation.

$$Cf = -1.2066 - 1.1172\, We - 0.3298\, Mg + 0.1583\, Cs, \tag{17}$$

$$Nu = 0.3399 - 0.551 Q - 0.8342\, Ecn + 0.3175\, Pr, \tag{18}$$

$$Sh = 0.9639 - 0.194\, Eg + 0.8957 \Gamma. \tag{19}$$

Equation (17) shows that while an upsurge in *We* and *Mg* causes a decrease in the friction coefficient, an upsurge in *Cs* causes an increase in it. When *We* increases, the fluid exhibits increased elasticity and stronger internal stresses. This elasticity makes the fluid layers resist deformation and tend to stick together. As a result, the fluid offers less resistance to the overall flow, leading to a decrease in skin friction coefficient. The friction coefficient rises by 11.50% as the value of *Cs* ranges from 0.5 to 3. According to equation (18), an upsurge in Eckert number and heat source parameter causes the Nusselt number to decline, while a surge in Prandtl number causes the same to rise. Research has revealed that the Nusselt number experiences an increase of 33.65% when the Prandtl number falls between the range of 0.5 to 3.5. From equation (19), it is evident that there is a decrement in the mass transfer rate with the rise in activation energy parameter and an escalation in the same with the rise in the reaction rate parameter. It is observed that the Sherwood number rises by 20.02% as the value of *Eg* ranges from 0 to 3.

4. Conclusions

This study effectively examined the flow and thermal characteristics of a Ree-Eyring fluid on an elastic sheet using a numerical method. The analysis considered the impact of viscous dissipation, non-uniform heat source, and activation energy parameters. The major findings indicate that multiple parameters have a considerable impact on the various fluid flow features including heat transfer:

- A stronger magnetic field (higher parameter) reduces fluid velocity.
- A higher Ree-Eyring and couple stress parameters promote faster flow rates.
- The Eckert number and heat source parameter contribute to a rise in fluid temperature.

- A higher Prandtl number signifies stronger thermal diffusivity, resulting in a lower temperature profile.
- A higher Brinkman number indicates a more significant role for viscous dissipation, leading to increased entropy generation.
- It is observed that the Sherwood number rises by 20.02% as the value of Eg ranges from 0 to 3.

Acknowledgment

The authors thank their respective college managements for their support and encouragement.

Competing Interests

The authors declare that they have no competing interests.

Authors' Contributions

All the authors contributed significantly in writing this article. The authors read and approved the final manuscript.

References

[1] N. A. N. Ariffin, I. Waini, A. R. M. Kasim, M. H. A. Kamal, M. R. Ilias and S. A. Kechil, Flow and heat transfer analysis on Reiner-Philippoff fluid flow over a stretching sheet in the presence of first and second order velocity slip and temperature jump effects, *CFD Letters* **15**(1) (2023), 88 – 102, DOI: 10.37934/cfdl.15.1.88102.

[2] M. Arshad, A. Hussain, A. Hassam, P. Wróblewski, A. Elfasakhany, M. A. Elkotb, M. A. H. Abdelmohimen and A. M. Galal, Thermal energy investigation of magneto-hydrodynamic nano-material liquid flow over a stretching sheet: comparison of single and composite particles, *Alexandria Engineering Journal* **61**(12) (2022), 10453 – 10462, DOI: 10.1016/j.aej.2022.03.069.

[3] M. M. Biswal, K. Swain, G. C. Dash and K. Ojha, Study of radiative magneto-non-Newtonian fluid flow over a nonlinearly elongating sheet with Soret and Dufour effects, *Numerical Heat Transfer, Part A: Applications* **83**(4) (2023), 331 – 342, DOI: 10.1080/10407782.2022.2091379.

[4] S. Faghiri, S. Akbari, M. B. Shafii and K. Hosseinzadeh, Hydrothermal analysis of non-Newtonian fluid flow (blood) through the circular tube under prescribed non-uniform wall heat flux, *Theoretical and Applied Mechanics Letters* **12**(4) (2022), 100360, DOI: 10.1016/j.taml.2022.100360.

[5] A. Hussain, S. Akbar, L. Sarwar, S. Nadeem and Z. Iqbal, Effect of time dependent viscosity and radiation efficacy on a non-Newtonian fluid flow, *Heliyon* **5**(2) (2019), e01203, DOI: 10.1016/j.heliyon.2019.e01203.

[6] S. M. Ibrahim, P. V. Kumar and O. D. Makinde, Chemical reaction and radiation effects on non-Newtonian fluid flow over a stretching sheet with non-uniform thickness and heat source, *Defect and Diffusion Forum* **387** (2018), 319 – 331, DOI: 10.4028/www.scientific.net/DDF.387.319.

[7] A. S. Idowu and B. O. Falodun, Variable thermal conductivity and viscosity effects on non-Newtonian fluids flow through a vertical porous plate under Soret-Dufour influence, *Mathematics and Computers in Simulation* **177** (2020), 358 – 384, DOI: 10.1016/j.matcom.2020.05.001.

[8] T. Javed and A. Ghaffar, Numerical study of non-Newtonian Maxwell fluid in the region of oblique stagnation point flow over a stretching sheet, *Journal of Mechanics* **32**(2) (2016), 175 – 184, DOI: 10.1017/jmech.2015.94.

[9] K. A. Khan, A. R. Seadawy and A. Jhangeer, Numerical appraisal under the influence of the time dependent Maxwell fluid flow over a stretching sheet, *Mathematical Methods in the Applied Sciences* **44**(7) (2021), 5265 – 5279, DOI: 10.1002/mma.7107.

[10] S. Khan, M. M. Selim, A. Khan, A. Ullah, T. Abdeljawad, Ikramullah, and W. K. Mashwani, On the analysis of the non-Newtonian fluid flow past a stretching/shrinking permeable surface with heat and mass transfer, *Coatings* **11**(5) (2021), 566, DOI: 10.3390/coatings11050566.

[11] K. A. Khan, M. Vivas-Cortez, K. Ishfaq, M. F. Javed, N. Raza, K. S. Nisar and A.-H. Abdel-Aty, Exploring the numerical simulation of Maxwell nanofluid flow over a stretching sheet with the influence of chemical reactions and thermal radiation, *Results in Physics* **60** (2024), 107635, DOI: 10.1016/j.rinp.2024.107635.

[12] S. A. Lone, S. Anwar, A. Saeed and G. Bognár, A stratified flow of a non-Newtonian Casson fluid comprising microorganisms on a stretching sheet with activation energy, *Scientific Reports* **13**(1) (2023), Article number: 11240, DOI: 10.1038/s41598-023-38260-0.

[13] B. Mahanthesh, B. J. Gireesha, R. S. Gorla and O. D. Makinde, Magnetohydrodynamic three-dimensional flow of nanofluids with slip and thermal radiation over a nonlinear stretching sheet: A numerical study, *Neural Computing and Applications* **30** (2018), 1557 – 1567, DOI: 10.1007/s00521-016-2742-5.

[14] T. Maranna, S. M. Sachhin, U. S. Mahabaleshwar and M. Hatami, Impact of Navier's slip and MHD on laminar boundary layer flow with heat transfer for non-Newtonian nanofluid over a porous media, *Scientific Reports* **13** (2023), Article number: 12634, DOI: 10.1038/s41598-023-39153-y.

[15] C. M. Mohana and B. R. Kumar, Nanoparticle shape effects on MHD Cu–water nanofluid flow over a stretching sheet with thermal radiation and heat source/sink, *International Journal of Modern Physics B* **38**(10) (2024), 2450151, DOI: 10.1142/S0217979224501510.

[16] R. M. Muntazir, M. Mushtaq, S. Shahzadi and K. Jabeen, MHD nanofluid flow around a permeable stretching sheet with thermal radiation and viscous dissipation, *Proceedings of the Institution of Mechanical Engineers, Part C: Journal of Mechanical Engineering Science* **236**(1) (2022), 137 – 152, DOI: 10.1177/09544062211023094.

[17] V. S. Patil, P. P. Human and A. B. Patil, MHD Williamson nanofluid flow past a permeable stretching sheet with thermal radiation and chemical reaction, *International Journal of Modelling and Simulation* **43**(3) (2023), 185 – 199, DOI: 10.1080/02286203.2022.2062166.

[18] D. P. C. Rao, S. Thiagarajan and V. S. Kumar, Heat transfer in Darcy-Forchheimer flow of tangent hyperbolic fluid over an inclined plate with Joule heating, *Journal of Applied Mathematics and Computational Mechanics* **20**(3) (2021), 31 – 40, DOI: 10.17512/jamcm.2021.3.03.

[19] G. Rasool, A. Shafiq, C. M. Khalique and T. Zhang, Magnetohydrodynamic Darcy–Forchheimer nanofluid flow over a nonlinear stretching sheet, *Physica Scripta* **94** (2019), 105221, DOI: 10.1088/1402-4896/ab18c8.

[20] N. Rehman, R. Mahmood, A. H. Majeed, I. Khan and A. Mohamed, Multigrid simulations of non-Newtonian fluid flow and heat transfer in a ventilated square cavity with mixed convection and baffles, *Scientific Reports* **14** (2024), Article number: 6694, DOI: 10.1038/s41598-024-57322-5.

[21] Sajjad-ur-Rehman, Rizwan-ul-Haq, C. Lee and S. Nadeem, Numerical study of non-Newtonian fluid flow over an exponentially stretching surface: an optimal HAM validation, *Journal of the Brazilian Society of Mechanical Sciences and Engineering* **39** (2017), 1589 – 1596, DOI: 10.1007/s40430-016-0687-3.

[22] K. Sarada, R. J. P. Gowda, I. E. Sarris, R. N. Kumar and B. C. Prasannakumara, Effect of magnetohydrodynamics on heat transfer behaviour of a non-Newtonian fluid flow over a stretching sheet under local thermal non-equilibrium condition, *Fluids* **6**(8) (2021), 264, DOI: 10.3390/fluids6080264.

[23] M. H. Shahzad, A. U. Awan, A. Akgül, S. Nadeem, K. Guedri, M. K. Hassani and B. M. Makhdoum, Analytical investigation of Carreau fluid flow through a non-circular conduit with wavy wall, *Scientific Reports* **14**(1) (2024), Article number: 2437, DOI: 10.1038/s41598-024-52848-0.

[24] M. H. Shahzad, S. Nadeem, A. U. Awan, S. A. Allahyani, N. A. Ahammad and S. M. Eldin, On the steady flow of non-newtonian fluid through multi-stenosed elliptical artery: A theoretical model, *Ain Shams Engineering Journal* **15**(1) (2024), 102262, DOI: 10.1016/j.asej.2023.102262.

[25] R. P. Sharma and S. Shaw, MHD non-Newtonian fluid flow past a stretching sheet under the influence of non-linear radiation and viscous dissipation, *Journal of Applied and Computational Mechanics* **8**(3) (2022), 949 – 961, DOI: 10.22055/jacm.2021.34993.2533.

[26] P. Sreedevi, P. S. Reddy and A. Chamkha, Heat and mass transfer analysis of unsteady hybrid nanofluid flow over a stretching sheet with thermal radiation, *SN Applied Sciences* **2**(7) (2020), 1222, DOI: 10.1007/s42452-020-3011-x.